Differences in the Transient Kinetics of the Binding of D-ADP and its Mirror Image L-ADP to Human 3-Phosphoglycerate Kinase Revealed by the Presence of 3-Phosphoglycerate†

Claire Gondeau,‡ Laurent Chaloin,‡ Andrea Varga,§ Béatrice Roy,|| Perrine Lallemand,‡ Christian Périgaud,|| Tom Barman,‡ Mária Vas,§ and Corinne Lionne*,‡

Centre d'tudes d'agents Pathogènes et Biotechnologies pour la Santé (CPBS), UMR 5236, CNRS-Université Montpellier 1-Université Montpellier 2, Institut de Biologie, 4 bd Henri IV, CS69033, 34965 Montpellier cedex 2, France, Institute of Enzymology, Biological Research Center, Hungarian Academy of Sciences, Karolina Str. 29, H-1113 Budapest, Hungary, Institut des Biomolécules Max Mousseron (IBMM), UMR 5247, CNRS-Université Montpellier 1-Université Montpellier 2, case courrier 1705, Université Montpellier 2, Place Eugène Bataillon, 34095 Montpellier cedex 5, France

Received November 22, 2007; Revised Manuscript Received January 11, 2008

ABSTRACT: L-Nucleosides comprise a new class of antiviral and anticancer agents that are converted in vivo by a cascade of kinases to pharmacologically active nucleoside triphosphates. The last step of the cascade may be catalyzed by 3-phosphoglycerate kinase (PGK), an enzyme that has low specificity for nucleoside diphosphate (NDP): NDP + 1,3-bisphosphoglycerate ↔ NTP + 3-phosphoglycerate. Here we compared the kinetics of the formation of the complexes of human PGK with D- and its mirror image L-ADP and the effect of 3-phosphoglycerate (PG) on these by exploiting the fluorescence signal of PGK that occurs upon its interaction with nucleotide substrate. Two types of experiment were carried out: equilibrium (estimation of dissociation constants) and stopped-flow (transient kinetics of the interactions). We show that under our experimental conditions (buffer containing 30% methanol, 4 °C) PGK binds D- and L-ADP with similar kinetics. However, whereas PG increased the dissociation rate constant for D-ADP by a factor of 8—which is a kinetic explanation for "substrate antagonism"—PG had little effect on this constant for L-ADP. We explain this difference by a molecular modeling study that showed that the β-phosphates of D- and L-ADP have different orientations when bound to the active site of human PGK. The difference is unexpected because L-ADP is almost as catalytically competent as D-ADP [Varga, A. et al. (2008) *Biochem. Biophys. Res. Commun. 366*, 994–1000].

Analogues of nucleotide triphosphates form an important group of drugs for combating certain viral diseases and cancers (refs *1–3* and references cited therein). Because nucleotides do not pass the cytoplasmic membrane, they cannot be used directly as drugs; instead they are given as the corresponding nucleosides because these "prodrugs" do pass. Upon entry into the cell, the nucleoside prodrug is phosphorylated by a cascade of cellular kinases to the corresponding mono-, di- and, finally, the pharmacologically active triphosphate (*4, 5*). Here, we are concerned with the last step of the cascade, that is, nucleoside di- to triphosphate. This is thought to involve kinases of low specificity for the nucleotide diphosphate substrate such as nucleoside diphosphate kinase, pyruvate kinase, and in particular 3-phosphoglycerate kinase (PGK[1]; EC 2.7.2.3) (*6, 7*).

L-Nucleoside analogue prodrugs are of special interest as a new class of antiviral and anticancer agents (reviewed in ref *8*). For example, it has been shown that several L-nucleotides possess better anti-HIV properties than the corresponding D-isomer (*9–11*). L-Nucleosides are the mirror images of the natural D-nucleosides. Certain enzymes lack enantioselectivity for nucleotides, whereas others will only use the D-isomer (*11, 12*). Verri et al. (*12*) addressed the question of this unexpected activity by proposing that because L-nucleotides do not appear to occur naturally, the enantioselectivity of enzymes "may only be a side property, depending more on chance than on evolution".

PGK catalyzes the reversible phosphotransfer between 1,3-bisphosphoglycerate (bPG) and MgADP: bPG + MgADP

* To whom correspondence should be addressed. Telephone: +33-467-600-595; fax: +33-467-604-420; e-mail: corinne.lionne@univ-montp1.fr.

† The present publication was prepared within the framework of the Hungarian-French Intergovernmental Scientific and Technological Cupertino Program and was supported by the grant from Egide (Balaton program No. 14100ZF) as well as by the Hungarian Foundation of Research and Innovative Technology (OMFB-00493/2007, Project No. F-43/2006). The financial support provided by grants from the "Agence Nationale de Recherches sur le Sida" and OTKA NI 61915 from the Hungarian National Research Foundation as well as by European Community − Research Infrastructure Action under the FP6 "Structuring the European Research Area Programme" (contract No. RII3-CT-2004–506008) are also gratefully acknowledged. Andrea Varga was supported by a short-term FEBS fellowship.

‡ Centre d'tudes d'agents Pathogènes et Biotechnologies pour la Santé (CPBS), CNRS-Universités Montpellier 1 et 2.

§ Hungarian Academy of Sciences.

|| Institut des Biomolécules Max Mousseron (IBMM), CNRS-Universités Montpellier 1 et 2.

[1] Abbreviations: bPG, 1,3-bisphosphoglycerate; PG, 3-phosphoglycerate; PGK, 3-phosphoglycerate kinase; HIV, human immunodeficiency virus; hPGK, human 3-phosphoglycerate kinase; yPGK, yeast 3-phosphoglycerate kinase.

10.1021/bi7023145 CCC: $40.75
Published on Web 02/21/2008

↔ PG + MgATP and is expressed in all tissues and living organisms studied so far. The sequences of mammalian PGKs are conserved at more than 96%. The crystal structure of horse muscle PGK (apoenzyme) has been solved (*13, 14*). The binary complexes PGK•PG (*15*) and PGK•MgATP (*16*) and the ternary complexes PGK•PG•MnAMP-PNP (*17*), PGK•PG•MgADP (*18*), and PGK•PG•MgAMP-PCP (*19*) have been described for pig PGK (see ref *20* for other structures). The structure of human PGK (hPGK), the enzyme studied in this work, has not yet been resolved.

PGK is a monomer protein that contains two globular domains. The N-terminal domain contains a basic region that binds bPG or PG, and the C-terminal domain contains the nucleotide-binding site. In the apoenzyme, the substrate binding sites are too far apart to allow phospho-transfer, but upon the bending of both substrates, it is thought that the two domains undergo an extensive "hinge binding motion" that leads to the approximation of the sites (*14*). The closure of the two domains has been demonstrated by two independent crystal structures, namely those of *Trypanosoma brucei* (*21*) and *Thermotoga maritima* (*22*) PGKs.

The nucleotide specificity of PGK has been reviewed (*6, 7, 23*). In general, PGK works better with purine- rather than pyrimidine-based nucleotides. Human PGK exhibits low enantioselectivity toward its nucleotide substrates. Krishnan et al. (*24*) showed that HelaS3 and 2.2.15 cells possess significant activities toward L-nucleoside analogues. Accordingly, when the hPGK activity of these cells was down-regulated by siRNA, there was a decrease in the formation of the analogue triphosphates. Gallois-Montbrun et al. (*23*) showed that hPGK has broad specificity toward antiviral nucleoside analogues. In particular, they showed that hPGK uses both D- and L-ATP as substrates. Thus, at 25 °C with L-ATP, $k_{cat} = 100\ s^{-1}$ and $K_m = 0.3$ mM and with D-ATP, 500 s^{-1} and 0.5 mM, respectively (pH 7.5 and with 50 mM sodium sulfate). Very recently, Varga et al. (*25*) compared the mode of interaction of D- and L-ADP with hPGK and obtained the steady state parameters in the direction of ATP formation. At 25 °C, with L-ADP, $k_{cat} = 685\ s^{-1}$ and $K_m = 0.27$ mM; with D-ADP, $k_{cat} = 1085\ s^{-1}$ and $K_m = 0.12$ mM.

As a first attempt at understanding the mechanism of action of hPGK on non-natural L-nucleoside diphosphates, we compared the kinetics of the formation of the binary complexes of hPGK with D- and L-ADP and the effect of PG upon these kinetics. With D-ADP, the unproductive E•PG•D-ADP is formed in the presence of PG and, as pointed out by several workers (*21, 26–29*), studies on this model of the functioning ternary complex have provided important information on the modes of binding of the substrates to PGK. However, these works refer mainly to PGK from sources other than human. Further, there is no information on a putative E•PG•L-ADP from any PGK.

As with yeast PGK (*30, 31*), the study was carried out at 4 °C and in a buffer containing 30% methanol to decrease the rapidity of the kinetics. We show that, whereas the two binary complexes are formed with similar kinetics, the interactions of D-ADP and L-ADP with hPGK in the presence of PG are different.

MATERIALS AND METHODS

Protein and Reagents. Recombinant hPGK was produced in BL21 (DE3)/pDIA17 *E. coli* cells transformed with the pgk-pET28a plasmid, kindly provided by D. Deville-Bonne (FRE 2852 Université Paris VI, France). The 6His-tagged human PGK was purified from the BL21 cell lysate according to Gallois-Montbrun et al. (*23*). Briefly, cells expressing PGK were lysed with a Cell Disruptor Z Plus series (Constant System Ltd., United Kingdom) in a lysis buffer (50 mM NaH_2PO_4, 300 mM NaCl, 10 mM imidazole, complete EDTA-free, pH 8.0). The clarified lysate was applied onto a nickel affinity column equilibrated in the lysis buffer and extensively washed. The PGK was eluted with a linear gradient of imidazole (10–250 mM imidazole in the lysis buffer at pH 8.0). The fractions containing PGK were pooled, concentrated up to 50 mg/mL, dialyzed against a buffer containing 50 mM Tris-HCl pH 7.5, 20 mM NaCl, 1 mM DTT, and 50% glycerol, and stored at −20 °C. The concentration of the 99% pure protein was determined using an extinction coefficient of 28 335 $M^{-1}\ cm^{-1}$ at 280 nm. The presence of the 6His-tag had no effect on the catalytic activity of PGK (results not shown).

L-AMP was synthesized by selective phosphorylation of L-adenosine as described previously (*32*). Solid 1,1′-carbonyldiimidazole (486 mg, 3 mmol) was added to a stirred solution of the tri-*n*-butylammonium salt of L-AMP (266 mg, 0.5 mmol) in anhydrous dimethylformamide (DMF, 10 mL) at room temperature under argon. The course of phosphorimidazolate formation was followed by ^{31}P NMR (appearance of a singlet at δ −10.42 ppm in DMSO-d_6). The reaction mixture was stirred for 3 h at room temperature, after which methanol (150 μL) was added. After 30 min, a solution of tri-*n*-butylammonium phosphate (707 mg, 2.5 mmol) in 5 mL of DMF was added. The reaction was controlled by TLC using 2-propanol/NH_4OH/water 11/7/2. The solution was stirred for 1 day at room temperature. The solvent was then evaporated under reduced pressure to give a residue that was diluted with water and purified by ion exchange chromatography using a DEAE-Sephadex A-25 (elution: gradient of TEAB pH 7.5 from 10 mM to 1 M), followed by chromatography on a RP18 (elution with water). The triethylammonium cation was then exchanged for a sodium cation by passing the nucleotide solution through a DOWEX-AG 50WX2–400 column, the purified fractions were lyophilized to give 117 mg of L-ADP (yield 50%). Its physicochemical properties were in accordance with literature (*32*).

Experimental Conditions. The buffer contained 20 mM triethanolamine, pH 7.5, 0.1 M potassium acetate, and 1 mM free Mg^{2+}, as magnesium acetate. Thus, unless otherwise stated, in our experiments "ADP" refers to Mg^{2+}-ADP. As specified in the figure legends and tables, experiments were also carried out in the same buffer that contained 30% (v/v) methanol. The concentrations of PGK, ADP, and PG in the figure legends or in the text refer to the final reaction mixture concentrations. The temperature was 4 °C.

PGK Activity by a Coupled Enzyme System. The PGK reaction was followed in the reverse direction (bPG formation) by coupling to glyceraldehyde-3-phosphate dehydrogenase as previously described (*30, 33*).

Equilibrium Fluorescence Spectroscopy. Experiments were carried out on a Xenius spectrofluorimeter (Safas, Monaco).

Table 1: Comparison of the Affinities of hPGK for Different Ligands in Buffer With or Without Methanol[a]

ligands		no methanol		30% methanol	
variable	constant	ΔF (%)	K_d (μM)	ΔF (%)	K_d (μM)
D-ADP		-16.3 ± 0.5	13 ± 2	-12.2 ± 0.5	7.7 ± 0.6
D-ADP	250 μM PG	-23.5 ± 0.5	60 ± 3	-20.2 ± 0.4	50 ± 3
L-ADP		-14.3 ± 0.5	21 ± 2	-14.3 ± 0.3	17 ± 1
L-ADP	250 μM PG	-15.5 ± 0.8	34 ± 3	-18.8 ± 0.6	28 ± 2
PG		4.3 ± 0.4	3.9 ± 1.4	7.4 ± 0.4	0.7 ± 0.2
PG	150 μM D-ADP	nd	nd	6.2 ± 0.4	6.5 ± 0.7
PG	150 μM L-ADP	nd	nd	7.2 ± 0.4	3.5 ± 0.7

[a] The K_d values were determined by equilibrium fluorescence spectroscopy (Figure 1); conditions: 20 mM triethanolamine, pH 7.5, 0.1 M potassium acetate, 1 mM free Mg^{2+}, with or without 30% methanol, and at 4 °C. nd, not determined.

Table 2: Effect of PG on the Transient Kinetics of the Binding of D- and L-ADP to hPGK in Methanol Containing Buffer at 4 °C[a]

$$E(\cdot PG) + ADP \underset{k_{off}}{\overset{k_{on}}{\rightleftharpoons}} E^*(\cdot PG)\cdot ADP$$

$$E(\cdot PG) + ADP \overset{K_1}{\rightleftharpoons} E(\cdot PG)\cdot ADP \underset{k_{-2}}{\overset{k_2}{\rightleftharpoons}} E^*(\cdot PG)\cdot ADP$$

		ADP binding kinetics[b]			
ligand		transient kinetics (Figures 4 and 6)			equilibrium (Figures 1 and 2)
variable	constant[c]	$k_{on} = k_2/K_1$ (μM^{-1} s^{-1})	$k_{off} = k_{-2}$ (s^{-1})	$k_{off}/k_{on} = K_1K_2$ (μM)	$K_d = K_1K_2/(1 + K_2)$ (μM)
D-ADP		6.1 ± 0.3	38 ± 10	6.2	7.7
D-ADP	PG	4.6 ± 0.6	313 ± 40	68	50
L-ADP		3.1 ± 0.2	55 ± 6	18	17
L-ADP	PG	2.4 ± 0.2	79 ± 10	33	28

[a] The values of k_{on} and k_{off} were obtained from the k_{obs} vs ADP concentration dependences (Figure 6). For experimental details, see the legend to Figure 1 and the text. [b] $K_i = k_{-i}/k_i$. [c] The concentration of PG was 200 μM in transient kinetic experiments and 250 μM in equilibrium studies.

The formation of the binary PGK·PG or PGK·ADP complex was followed by measuring the tryptophan fluorescence change of a solution of PGK (initially at 2.5 μM) mixed with increasing concentrations of PG or ADP, respectively. The formation of the ternary complex PGK·PG·ADP was followed using an initial solution containing 2.5 μM PGK and 250 μM PG or 150 μM ADP and adding increasing amounts of ADP or PG, respectively.

The volume of substrate added to the enzyme solution was less than 10% of the initial volume to limit the dilution of PGK. The effect of a 10% dilution of the PGK solution with buffer had no effect on its fluorescence corrected for the change in concentration (not shown). The titrations were performed in a 1 cm path-length cuvette. The excitation and emission wavelengths were 295 and 335 nm, respectively, with a 10 nm bandwidth for both the excitation and emission monochromators.

The dissociation constants (K_d) for the substrates of PGK were determined by fitting the intrinsic PGK fluorescence variation as a function of the substrate concentration using the GraFit program (v3.03, Ericathus Software Limited, Staines, United Kingdom) and the following quadratic equation (eq 1),

$$\Delta F = \frac{\Delta F_{max}}{[PGK]_0} \times \left[\left(([S]_0 + [PGK]_0 + K_d) - \sqrt{([S]_0 + [PGK]_0 + K_d)^2 - 4[S]_0[PGK]_0}\right)/2\right] \quad (1)$$

where ΔF is the variation of fluorescence intensity corrected for the dilution of the protein solution, ΔF_{max} is the extrapolated maximal variation of fluorescence, and $[S]_0$ and $[PGK]_0$ are the total concentrations of the substrate and enzyme, respectively.

Stopped-flow Experiments. The kinetics of the interaction of PGK with its substrates was studied by monitoring the tryptophan fluorescence variation of the PGK upon binding in a stopped-flow apparatus (SF-61 DX2, TgK Scientific, United Kingdom). The dead time of this apparatus is 0.5 ms. The excitation wavelength was 295 nm, and emission was >320 nm using a cutoff filter (WG320 from TgK Scientific). The bandwidth for excitation was 2 nm. The fluorescence of the PGK solution or a mixture of PGK with a fixed concentration of PG was set as 100%. For each experimental condition, a series of 5–12 shots were carried out and averaged. Fluorescence changes time courses were fitted with GraFit using a single exponential equation (eq 2):

$$F = F_0 - \Delta F \times \exp(-k_{obs}t) \quad (2)$$

where t is the time after mixing PGK solution with the substrate in the stopped-flow apparatus, F is the observed fluorescence at time t, F_0 is the initial fluorescence intensity (at time $t = 0$), ΔF is the variation of fluorescence at $t = \infty$, and k_{obs} is the observed rate constant for the change of fluorescence.

Errors. The errors given by the computer analysis of the raw data are indicated in Tables 1 and 2. These do not take into account of the potentially larger experimental errors (*31*).

Molecular Modeling and Docking of D-ADP and L-ADP to hPGK. Models of the 3D structures of hPGK in the open and closed conformations were built from pig muscle PGK (1VJC and 1VJD, open) and *T. brucei* PGK (13PK, closed) crystal structures using the Modeler release program 8v2 (*34*). The sequences of pig and hPGK are 97% identical, so

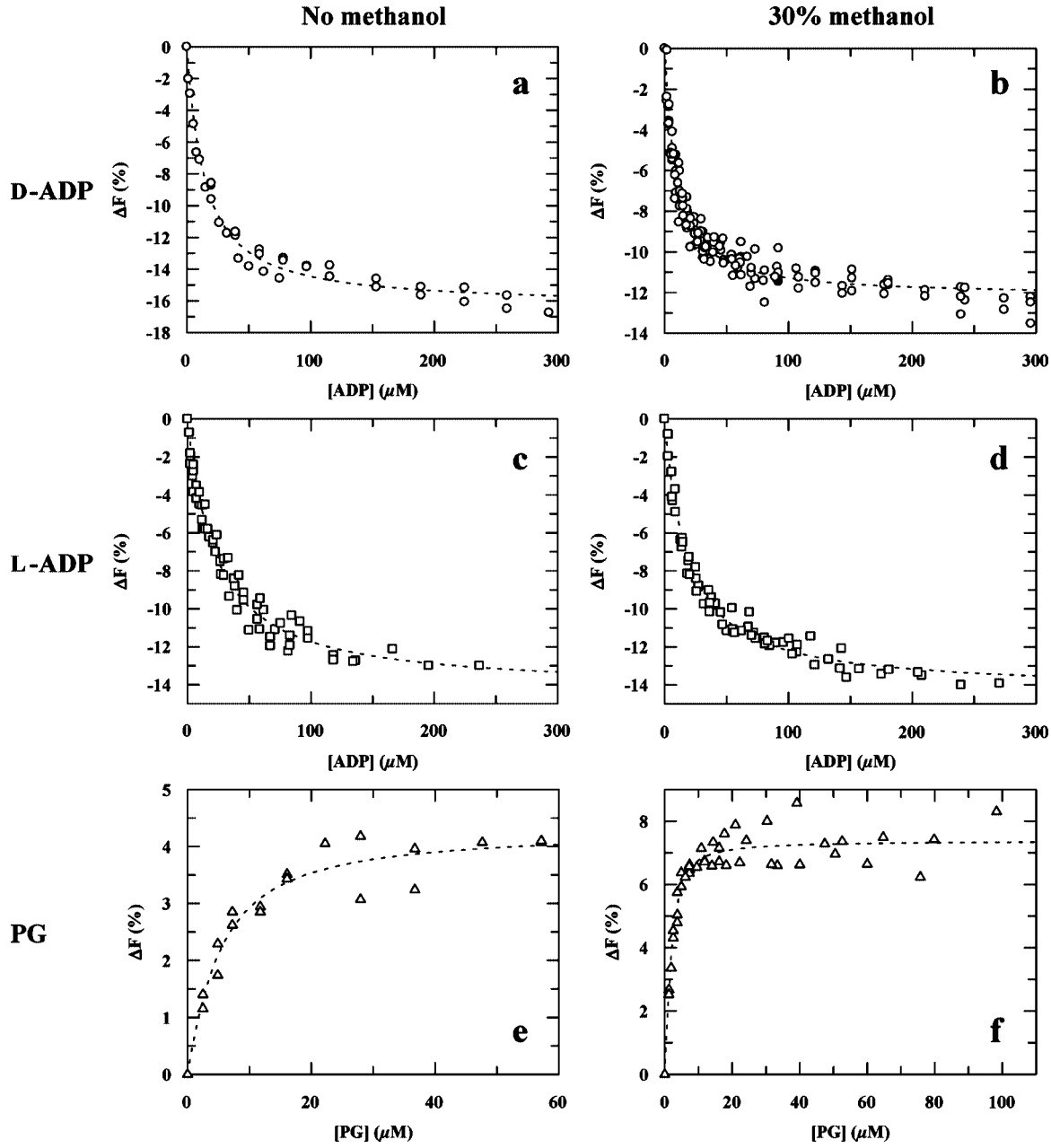

FIGURE 1: Equilibrium studies: dependences of the amplitude of the substrate-induced tryptophan fluorescence change of hPGK on the D-ADP (○, a, b), L-ADP (□, c, d), or PG (Δ, e, f) concentrations in buffer without (a, c, e) or with 30% methanol (b, d, f). The initial concentration of PGK was 2.5 μM. The data were fitted using equation eq 1, and the values obtained for ΔF_{max} and K_d are in Table 1.

the program was used directly for the building of the open model. For modeling the closed conformation of hPGK, a graphical alignment method based on the different crystal structures of PGK from yeast, pig, horse, and *T. brucei* was used to improve the quality of the model. Because the sequence identity of human and *T. brucei* is only 43%, this artifice was essential to obtain information on all folded and functional regions of the enzyme. All hydrogen atoms were added to the model, including those that define the correct ionization state of histidine, using the hbuild command of Charmm program (Harvard University). The VMD program (*35*) was used to analyze the interactions and to measure the distances between the atoms in the hPGK model and bound D-ADP or L-ADP.

Docking of D- or L-ADP into the hPGK model was carried out by the use of GOLD (Genetic Optimization for Ligand Docking, CCDC software limited), v3.2 that uses a genetic algorithm (GA). This method permits a certain amount of flexibility: partial with the protein and complete with the ligand. For each of the 50 independent GA runs, a default maximum number of 100 000 genetic operations was performed, using default operator weights and a population size of 100 chromosomes. In other words, the possible docked orientations of the ligand are defined as chromosomes that belong to a given population. This population can evolve like human beings, including crossover, migration, or point mutation, designated hereafter as "genetic operations" that are modulated by the operator weight.

The atom chosen as target to define the nucleotide binding site was the nitrogen atom of Pro338 with an active site radius of 15 Å in combination with scrutiny for a cavity. The magnesium ion was coordinated with a tetrahedral geometry with the two oxygen atoms of Asp374 and two water molecules. The Mg-ion should be coordinated with 6

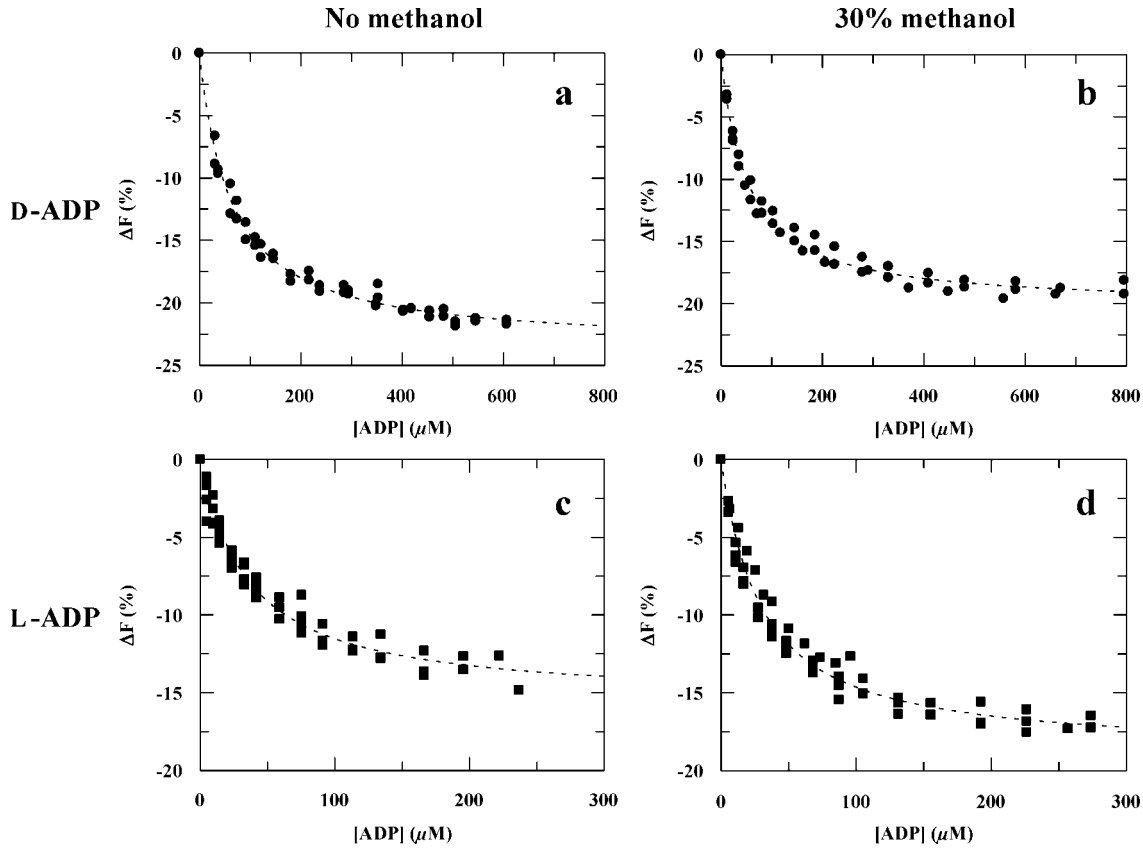

FIGURE 2: Equilibrium studies: effect of PG on the dependences of the amplitude of the substrate-induced tryptophan fluorescence change of human PGK on the D-ADP (●, a, b) or L-ADP (■, c, d) concentrations in the presence of PG, in buffer without (a, c) or with 30% methanol (b, d). The initial concentration of hPGK was 2.5 μM, and that of PG was 250 μM. The data were fitted using eq 1, and the values obtained for ΔF_{max} and K_d are in Table 1.

ligands, as can be clearly seen in the 1.6 Å resolution crystal structure of the MgADP binary complex of *Bacillus stearothermophilus* PGK [1PHP, (*36*)]. When the resolution of the X-ray structure is not high enough, not all ligands of Mg-ion can be seen, and in the present modeled structure two water molecules could be missing.

Chemscore was used as a scoring function for all docking, and the conformation of the solutions that ranked best was analyzed further following energy minimization. Briefly, the potential energy was minimized in three steps using the Charmm program (500 steps of steepest descent followed by 5,000 steps of conjugate gradient with a tolerance of 0.01 kcal/mol·Å). During this procedure, two distance restraints were imposed—one between the Mg^{2+} ion and Asp374 and the other between Glu343 and the two hydroxyl groups of the ribose. This was important to maintain the location of the substrate as obtained by the docking. All nonbonded interactions were calculated up to an interatomic distance of 10 Å, and interactions between 10 and 14 Å were approximated with a switching function (*37*).

For the docking of PG, the same strategy was followed, using the GOLD program, except that the target atom was the α-carbon of Gly166. A distance constraint between Asn25 (γ-carbon) and PG (oxygen atom of C2) was also included to optimize the orientation of PG at its binding site. This docking procedure was validated by the use of the structure of *T. brucei* PGK for which the PG binding site is known (*21*). For modeling the ternary complexes, PG was docked first and then ADP.

RESULTS AND DISCUSSION

When ATP, ADP, or PG binds to yeast PGK (yPGK), there is a change in the inherent fluorescence of the enzyme (*30*), a change that also occurs with hPGK. Here, we exploited this signal to carry out two types of experiment: equilibrium fluorescence (which allowed us to obtain estimates for the dissociation constants (K_d) for the ligands) and fluorescence stopped-flow (from which the transient kinetics of the binding processes were obtained). Because of the rapidity of the kinetics of the binding processes (*30, 38*), experiments were carried out at 4 °C and, to further increase the time resolution, in a buffer that contained 30% methanol.

Effect of Methanol on the Overall PGK Reaction (bPG Formation). When 30% methanol was included in the assay buffer with yPGK, both k_{cat} and K_m for ATP were reduced: 7.6 s^{-1} (from 72 s^{-1}) and 62 μM (from 109 μM), respectively (*30*). The presence of methanol had a similar effect on the steady state parameters with hPGK: $k_{cat} = 5.7$ s^{-1} from 38 s^{-1} and K_m for ATP 30 μM from 103 μM.

Equilibrium Fluorescence Experiments. The effect of the concentration of D-ADP on the amplitude of the fluorescence signal in the absence or presence of 30% methanol is illustrated in Figure 1, panels a and b. The data were fitted to eq 1, and the dissociation constants obtained are in Table 1.

As with D-ADP, when L-ADP was added to hPGK, there was a decrease in the fluorescence signal (Figures 1c and 1d). The amplitude of the signal was similar to that observed with D-ADP, which suggests that L-ADP binds to the same

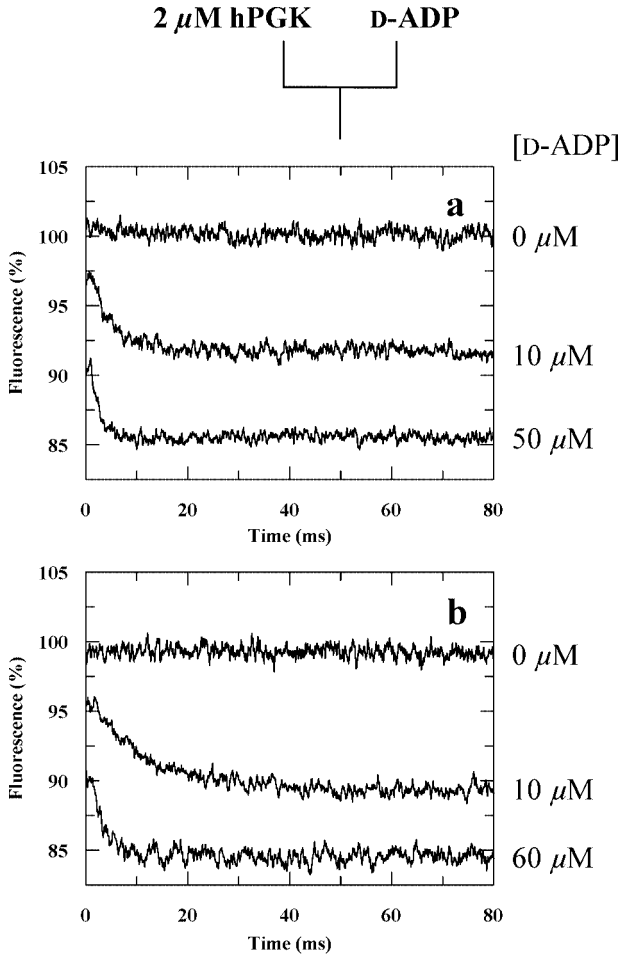

FIGURE 3: Transient kinetic studies: time courses of hPGK tryptophan fluorescence change induced by D-ADP (a) in buffer without methanol at 0, 10, or 50 μM D-ADP and (b) in buffer with 30% methanol at 0, 10, or 60 μM D-ADP. The transients were fitted to single exponentials (not shown) of kinetics, k_{obs}, (a) 257 s^{-1} at 10 μM and 775 s^{-1} at 50 μM and (b) 100 s^{-1} at 10 μM and 395 s^{-1} at 60 μM.

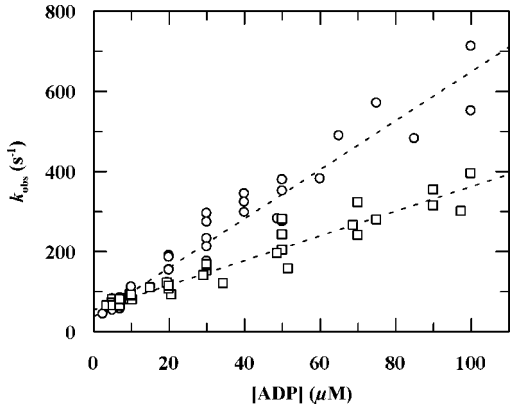

FIGURE 4: Dependences of k_{obs} on the concentration of D-ADP (○) and L-ADP (□) in buffer with 30% methanol. The data were fitted to straight lines each of slope k_2/K_1 and intercept on the k_{obs} axis k_{-2}. For estimates of the constants, see Table 2 and the text.

site as D-ADP. The dissociation constant for L-ADP was greater than that for D-ADP, whether or not the buffer contained methanol (Table 1).

As seen in Figure 2, panels a and b, and in Table 1, 250 μM PG significantly reduced the affinity of hPGK for D-ADP. Further experiments (not illustrated) showed that the K_d for ADP increased with the PG concentration to a limiting

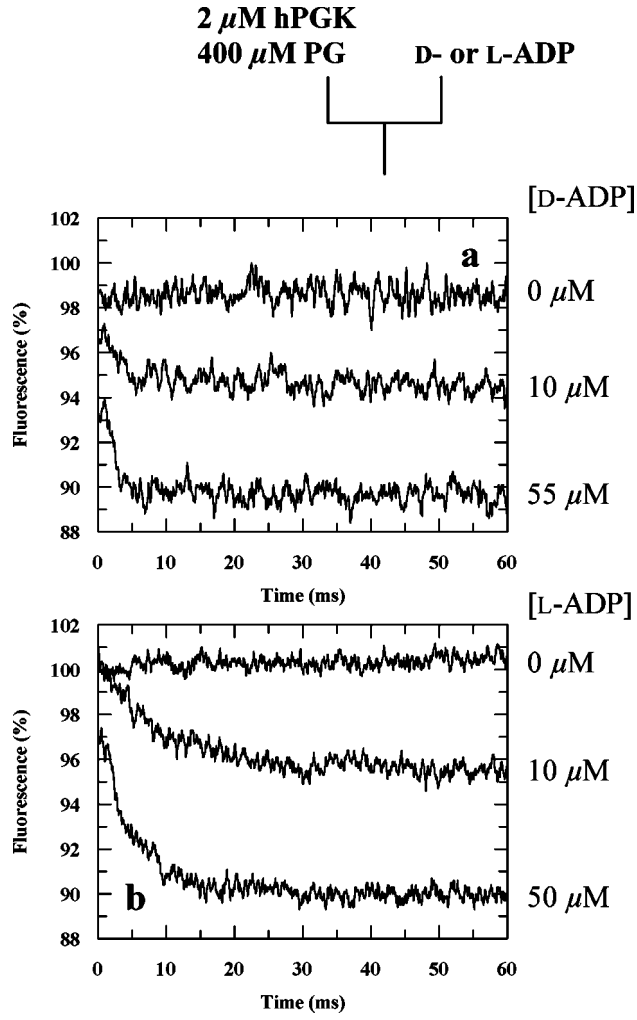

FIGURE 5: Effect of PG on the transient hPGK fluorescence kinetics induced by D-ADP (a) or L-ADP (b) in buffer with 30% methanol. The transients were fitted to single exponentials (not shown) of kinetics, k_{obs}, (a) 345 s^{-1} at 10 μM and 576 s^{-1} at 55 μM and (b) 106 s^{-1} at 10 μM and 210 s^{-1} at 50 μM.

plateau at about 200 μM in the methanol-free buffer and 100 μM in the methanol containing buffer.

In contrast to the situation with D-ADP, PG has only a small effect on the K_d for L-ADP (Figure 2, panels c and d; Table 1). Increasing the PG concentration up to 1 mM had no further detectable effect (data not illustrated). We note that the effects of PG on the dissociation constants for both D- and L-ADP were observed whether or not the buffer contained methanol.

The interaction of PG with hPGK leads to an increase of the fluorescence signal, but the amplitude of this was low, especially in the methanol-free buffer (Figure 1, panels e and f); nevertheless, it was possible to obtain estimates for the dissociation constant for PG (Table 1). It is noteworthy that with yPGK the fluorescence signal decreased upon the addition of PG (*30*).

It is thought that the binding of ATP and PG to PGK is random [e.g., refs *38, 39*], and if we assume that ADP and PG also bind in a random manner, then we can summarize the formation of the "abortive" E·PG·ADP by the thermodynamic box in Scheme 1 where E is hPGK; K_{PG1}, K_{ADP1}, K_{PG2}, and K_{ADP2} are dissociation constants, and $K_{ADP2}/K_{ADP1} = K_{PG2}/K_{PG1}$.

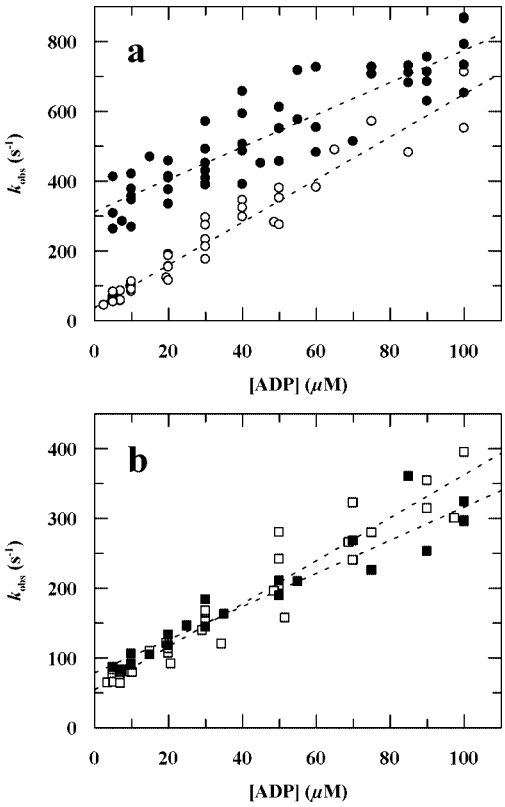

FIGURE 6: Effect of PG on the dependences of k_{obs} on the D-ADP (a) or L-ADP (b) concentration. In both (a) and (b) the open symbols are without PG, and the closed symbols are with 200 μM PG. The kinetic parameters obtained (slopes, k_2/K_1, and intercepts on the k_{obs} axis, k_{-2}) are summarized in Table 2.

Scheme 1

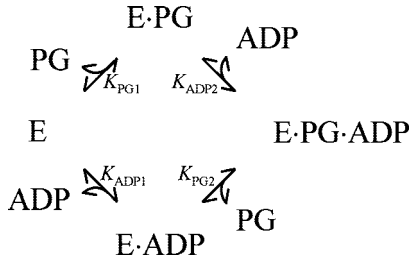

K_{PG1} and K_{ADP1} are the overall dissociation constants for PG and ADP, that is, for the formation of the corresponding binary complexes. K_{ADP2} and K_{PG2} are the dissociation constants for the formation of the ternary E•PG•ADP complex at saturation in PG or ADP, respectively (Table 1).

At constant [PG] and $\gg K_{PG1}$ and K_{PG2} and at variable ADP, Scheme 1 reduces to the following equations,

$$E \cdot PG + ADP \overset{K_{ADP2}}{\rightleftharpoons} E \cdot PG \cdot ADP \qquad (3)$$

and

$$\frac{\Delta F}{\Delta F_{max}} = \frac{[ADP]}{[ADP] + K_{ADP2}}$$

where ΔF is the fluorescence signal at [ADP] and ΔF_{max} is the signal at saturation in ADP.

From the dependence of $\Delta F/\Delta F_{max}$ on the D-ADP concentration at 250 μM PG (Figure 2b, Table 1), $K_{ADP2} = 50$ μM. Therefore, from the $K_{ADP2}/K_{ADP1} = K_{PG2}/K_{PG1}$ relationship and with $K_{ADP1} = 7.7$ μM and $K_{PG1} = 0.7$ μM, $K_{PG2} = 4.5$ μM, compared with 6.5 μM found experimentally. Thus, D-ADP reduces the affinity of hPGK for PG, and PG reduces that for D-ADP. This phenomenon of substrate antagonism has been discussed with pig PGK (*26, 27*) and has been observed with yPGK (*30*). For a further discussion on substrate antagonism, see CONCLUSIONS AND PROSPECTS section.

Scheme 2

$$E + ADP \underset{k_{off}}{\overset{k_{on}}{\rightleftharpoons}} E^*\cdot ADP$$

We now addressed the question of the cause of the effect of PG in reducing the affinity of hPGK for D-ADP: if we define K_{ADP1} as k_{off}/k_{on} (Scheme 2), is the antagonistic effect of PG due to a decrease in k_{on} or an increase in k_{off}? A way to answer this question is to obtain the details of the transient kinetics of the nucleotide binding, that is, to measure and define the rate constants k_{on} and k_{off} in the absence and presence of PG.

Fluorescence Stopped-flow Experiments. From the equilibrium binding studies, we conclude that the interactions of D- and L-ADP with hPGK are similar. However, their interactions in the presence of PG were different. We now set out to determine the kinetic causes for this difference by investigating the transient kinetics of the formation of the respective binary E•ADP and ternary E•PG•ADP complexes.

The kinetics of the observed decrease in fluorescence upon the addition of D-ADP to hPGK were difficult to measure, even by stopped-flow and at 4 °C, as illustrated in Figure 3a. The kinetics of the binding of D-ADP to yPGK were also very rapid (*30, 38*). A powerful way to reduce the rapidity of a kinetic process is to work under cryoenzymic conditions (*40*). This technique involves two perturbants: temperature and an antifreeze, usually an organic solvent. Its application may permit the accumulation of intermediates that cannot be obtained under standard conditions by slowing down the kinetics of their formation, by a change in a rate-limiting step or by shifts in equilibria. The mere addition of antifreeze may be enough to reduce the rapidity of a binding process. We have shown that, with yPGK in a buffer containing 30% methanol (v/v) and at 4 °C, the kinetics of the binding of ATP to the binary E•PG are reduced enough to allow their measurement.

Typical D-ADP-induced fluorescence transients in the methanol containing buffer at 4 °C are illustrated in Figure 3b. Each transient fitted well to an exponential of kinetics k_{obs} (eq 2).

The following control experiments were carried out to test the authenticity of these transient phases. First, when the enzyme was mixed with buffer alone, there was little change in fluorescence (Figure 3, at 0 μM ADP). Second, as summarized in Table 2, the dissociation constants estimated from the ADP dependences of the transient kinetics (see below) agree well with those obtained in the equilibrium experiments.

As illustrated in Figure 4, in 30% methanol the dependence of k_{obs} on the D-ADP concentration is linear up to 100 μM ADP of slope, $k_{on} = 6.1$ μM^{-1} s^{-1} and intercept on the k_{obs}

Scheme 3

$$E + ADP \overset{K_1}{\rightleftharpoons} E{\cdot}ADP \underset{k_{-2}}{\overset{k_2}{\rightleftharpoons}} E^*{\cdot}ADP$$

axis, $k_{off} = 38\ s^{-1}$ (see Treatment of Stopped-Flow Data section, below).

The kinetics of the fluorescence signal observed on the addition of L-ADP to PGK were similar to those with D-ADP under the same conditions (data not illustrated). As shown in Figure 4, the dependence of k_{obs} on the concentration of L-ADP could be fitted to a straight line of slope 3.1 μM^{-1} s^{-1} up to 100 μM L-ADP and an intercept on the k_{obs} axis of 55 s^{-1}.

Typical fluorescent time courses at different concentrations of D-ADP or L-ADP in the presence of 200 μM PG (final concentration) are illustrated in Figure 5. In these experiments, the enzyme had been preincubated with PG before the addition of ADP, as in the equilibrium studies.

A noteworthy feature of the experiments is that PG greatly increased the D-ADP binding kinetics. The increase was such that the amplitude of the measurable fluorescence signal was reduced, and k_{obs} was difficult to estimate with precision.

The dependence of k_{obs} on the D-ADP concentration is illustrated in Figure 6a, and estimates for the kinetic parameters (slope, k_{on}; intercept on the k_{obs} axis, k_{off}) are summarized in Table 2. From these results, it appears that in the presence of PG, the affinity of PGK for D-ADP decreases because there is an increase in the k_{off} for the nucleotide. The k_{on} seems to be little affected.

The authenticity of these results and conclusions was checked by obtaining D-ADP dependences on the same reaction mixtures but in (i) PGK mixed with (PG + D-ADP) and in (ii), (PGK + PG) mixed with (D-ADP + PG). The resulting dependences (data not illustrated) were very similar to that in Figure 6a. We also note that the system did not appear to be perturbed by merely mixing (PGK + PG) with buffer, as shown in Figure 5 (at 0 μM ADP).

The small effect of PG on the L-ADP binding was confirmed by transient kinetic experiments. The dependence of k_{obs} on the L-ADP concentration in the presence of 200 μM PG is shown in Figure 6b. It is noteworthy that, unlike with D-ADP, PG appears to have little effect on the L-ADP transient binding kinetics.

Treatment of Stopped-Flow Data. Is the ADP binding merely diffusion controlled ("one-step binding") as in Scheme 2, or does it also involve a protein isomerization process ("two-step binding") as in Scheme 3? Where ADP indicates the D- or L-enantiomer and the asterisk indicates an ADP-induced conformational change of PGK.

It is thought that ligands bind to enzymes in two steps [ref *41* and references cited therein], a situation that is in accord with the induced-fit theory of Koshland (*42, 43*). Here with hPGK, two further arguments support the two-step binding process in Scheme 3. First, the slope of the k_{obs} versus ADP dependence (Table 2 and Figure 4) is about 2 orders of magnitude too low to represent a one-step diffusion controlled process [e.g., ref *41*]. Second, there is evidence that the binding of ADP causes both local (*19, 36*) and global (*28, 44*) conformational changes of PGK; diffusion controlled reactions are assumed to occur without protein structural changes.

Therefore, we assume that ADP binds to PGK in two steps. Accordingly, from Scheme 3 we can write [e.g., ref *41*] eq 4.

$$k_{obs} = \frac{k_2[ADP]}{K_1 + [ADP]} + k_{-2} \quad (4)$$

This predicts that the dependence of k_{obs} versus [ADP] is hyperbolic, with an intercept on the k_{obs} axis of k_{-2} and a plateau of $k_2 + k_{-2}$. However, because of the rapidity of k_{obs} at high D-ADP concentrations, the plateau was not attained, and the experimentally obtained dependence was linear (Figure 4). Therefore, up to 100 μM ADP, $K_1 >$ [ADP] and eq 5 results.

$$k_{obs} = \frac{k_2[ADP]}{K_1} + k_{-2} \quad (5)$$

From Figure 4, with D-ADP, $k_2/K_1 = 6.1\ \mu M^{-1}\ s^{-1}$, $k_{-2} = 38\ s^{-1}$, and $K_1K_2 = 6.2\ \mu$M. If we apply Scheme 3 to the equilibrium experiments (*41*) to obtain eq 6.

$$K_{D\text{-}ADP1} = \frac{K_1K_2}{1 + K_2} = 7.7\,\mu M \quad (6)$$

The similarity of $K_{D\text{-}ADP1}$ and the K_1K_2 estimated in the transient kinetics experiments suggests that $K_2 \ll 1$, that is, $k_2 \gg k_{-2}$.

The slope of the k_{obs} versus [L-ADP] dependence is also too low to represent a diffusion controlled process, so it appears that, like D-ADP, L-ADP is bound in two steps to PGK, as in Scheme 3. Accordingly, with L-ADP, $k_2/K_1 = 3.1\ \mu M^{-1}\ s^{-1}$, $k_{-2} = 55\ s^{-1}$, and $K_1K_2 = 18\ \mu$M. Thus, as with D-ADP, with L-ADP K_2 appears to be <1.

In conclusion, these transient kinetic experiments confirm that L-ADP binds less strongly to hPGK than D-ADP.

The binding kinetics of both D- and L-ADP were determined in the presence of saturating concentrations of PG (closed symbols in Figure 6, panels a and b) and the rate constants obtained are summarized in Table 2. From these data, we conclude that whereas the k_{on} values for the two enantiomers are not significantly affected by PG, the kinetics of the release, k_{off}, of D-ADP are accelerated by PG but, interestingly, those of L-ADP are hardly affected. Thus, with D-ADP, the PG-induced increase in k_{off} could be an explanation for the phenomenon of substrate antagonism.

To conclude, in the presence of PG, there appears to be a significant difference in the kinetics of the interactions of D- and L-ADP with hPGK. We now consider a possible structural cause for this difference by a molecular modeling study of hPGK that involves a comparison of the docking of D- and L-ADP.

Comparison of the Mode of Binding of D- and L-ADP to hPGK: Molecular Modeling. The different behaviors of D- and L-ADP toward hPGK in the formation of the respective abortive E·PG·ADP complexes is surprising when one considers the overall steady state kinetics of the enzyme (*23, 25*).

Thus, we subjected the interaction contacts between hPGK and the different ligands to scrutiny by a docking procedure. We stress that this procedure is not "experimental"; it is based upon the assumptions that the E·ADP complexes are in the open conformation [by the use of the open pig PGK·D-ADP as a model (*16*)] and that the E·PG·ADP complexes are in

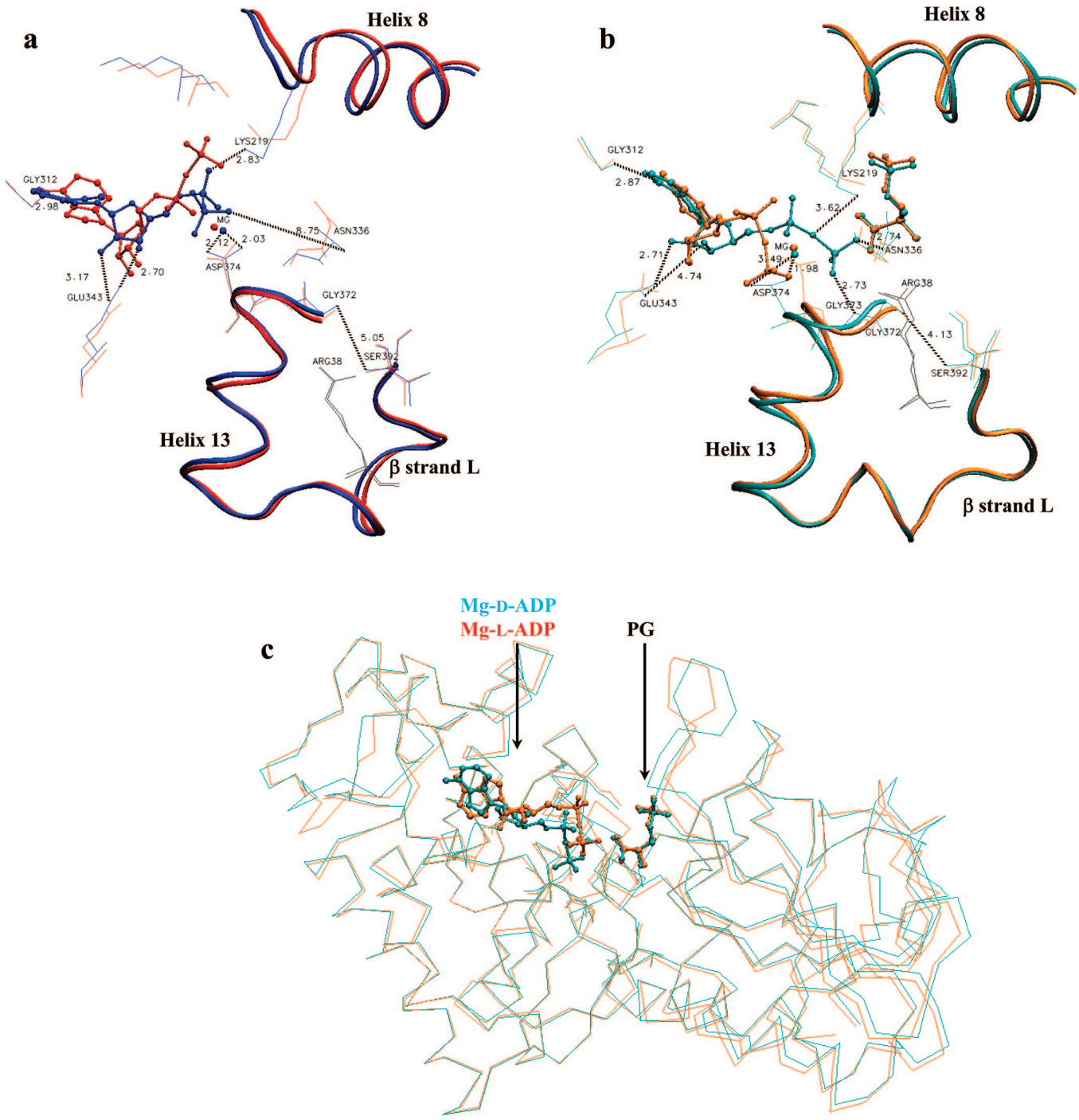

FIGURE 7: Docking of Mg-D-ADP (blue/cyan) or Mg-L-ADP (red/orange) in the nucleotide binding site of the two homology models of hPGK: open conformation for the binary complexes (a) and closed conformation with bound PG (b). The Cα-traces of the whole molecules with the bound ligands (ball and stick models) are shown in panel (c). Details of the ligand binding are illustrated by the atomic interactions (dashed lines) with the surrounding side-chains (stick models). Comparison of the distances between hPGK residues and the substrates are shown in Table 3 for all docked structures.

the closed conformation [by the use of the closed *T. brucei* PGK·PG·D-ADP as a model (*21*)].

As shown in Figure 7, panels a and b, L-ADP occupies the same binding site in the C-domain of hPGK as does D-ADP, independently of the conformational state of the enzyme. Several of the amino-acid residues that interact with the nucleotides are identical, for example, Gly312 and Glu343 (Table 3); however, in the presence of PG there are significant differences. Thus, in E·PG·D-ADP, in which E is in the closed conformation (Figure 7b), the β-phosphate of the ADP is H-bonded to Asn336 (located in β-strand J) and to the peptide N-atom of Gly373 (located in the positively charged N-terminus of α-helix 13). With L-ADP, the β-phosphate does not appear to interact with these highly conserved residues. However, with D- and L-ADP the β-phosphate interacts via a Mg^{2+} ion to Asp374 (in helix 13). When the structures of E·PG·D-ADP and E·PG·L-ADP are superimposed, the phosphates can be seen to occupy different positions, which leads to a small change in the position of helix 13. As a consequence, interdomain communication may be altered. Moreover, with D-ADP in the presence of PG, Asp374 is displaced; therefore, the Mg^{2+}

Table 3: Distances (Å) Between Substrates and Protein Residues in the Four Docked Structures[a] Shown in Figure 7

nucleotide groups	N6 (adenine)	2′-OH (ribose)	3′-OH (ribose)	Mg^{2+}	α-phosphate (oxygen)	β-phosphate (oxygen)	β-phosphate (oxygen)		β-phosphate
PG									1-C
hPGK residues	Gly312	Glu343	Glu343	Asp374	Lys219	Asn336	Gly373	Gly372(N)-Ser392(O)	
In Absence of PG									
D-ADP	2.98	3.17	2.70	2.03/2.12[b]	2.83	8.75	7.08	5.05	
L-ADP	2.87	2.73	2.70	2.00/2.03	2.70	8.83	10.00	4.89	
In Presence of PG									
D-ADP	2.87	2.71	4.74	**1.98/3.49**	3.62	2.74	2.73	4.13	**4.80**
L-ADP	3.44	2.68	2.73	**2.05/2.09**	7.07	7.41	5.50	3.76	**6.75**

[a] Open structure model used for the binary complexes and closed structure model for the ternary complexes. [b] The two values indicate distances of Mg^{2+} from the two O-atoms of Asp374 carboxylate.

ion is less connected to this residue, which leads to a weaker binding of Mg^{2+} ion to D-ADP. This observation is in good agreement with the suggestion of Merli et al. (*27*) that PG weakens the binding of D-ADP via the Mg^{2+} ion. From our docking results, the distance between the Mg^{2+} ion and the carboxylic group of Asp374 is increased upon PG binding with D-ADP but not with L-ADP (Table 3).

The different orientations of the β-phosphate in the two enantiomers seem to have an effect on the distance separating the phosphate and PG at the active site of the enzyme; with D-ADP the distance between the 1-C of PG and the β-phosphate is 4.80 Å, and with L-ADP the distance is 6.75 Å. With both nucleotides, the orientation of the two ligands leads to the proximation of two negatively charged oxygen atoms and therefore, we can not exclude a repulsive effect between the two ligands. This putative repulsion is especially strong with D-ADP, which would explain the effect of PG decreasing the affinity of hPGK for D-ADP. We note that the docking score with D-ADP is lower when PG is already bound to the enzyme.

However, repulsion between the two substrates would not be advantageous for catalysis. Instead, PG (through its indirect effect mediated by Arg38 toward βL and α13) weakens ligation of Mg^{2+} to Asp374. Thereby, the Mg^{2+} can move together with the nucleotide phosphate, and both can then occupy the optimal position for catalysis. Therefore, substrate antagonism appears to be an essential element of catalysis.

With L-ADP, even if the communication between the two substrate sites is weaker than with D-ADP, domain movement presumably still occurs because this enantiomer is catalytically active. This less effective domain communication could be the structural explanation for the somewhat reduced catalytic efficiency of hPGK toward L- with respect to D-purine based nucleotides (*23, 25*).

CONCLUSIONS AND PROSPECTS

Here we studied the kinetics of the interaction of D-ADP and L-ADP with hPGK. The use of a stopped-flow method based on the inherent tryptophan fluorescence of the enzyme enabled us to study, for the first time, the kinetics of formation of the binary E•D-ADP and E•L-ADP complexes. An important aspect of our work was to study the effect of PG on these kinetics; with D-ADP it is thought that the abortive E•PG•D-ADP is a good model for the catalytically important transient intermediate E•PG•D-ATP. Furthermore, by the use of this model one can study the phenomenon of substrate antagonism, in particular that the binding of the nucleotide substrate is weakened by PG (*45*). We propose two explanations for substrate antagonism: a PG-induced change in the interdomain communication of PGK that reduces Mg-Asp374 interaction or a repulsion of the two negatively charged substrates at the active site of PGK.

Merli et al. (*27*) pointed out the importance of Mg^{2+} in modulating the electrostatic interactions between nucleotide and PGK and, in particular, the effect of PG on these. PG appears to weaken the Mg^{2+} coordination of the β-phosphate of D-ADP, which leads to a reduction of the binding that facilitates its release. This could explain the PG-induced increase in the dissociation rate constant of D-ADP (k_{off}).

Substrate antagonism has been observed with phosphofructo-1-kinase, an enzyme that also has two negatively charged sustrates (*46, 47*). As with PGK, this enzyme binds its substrates in a random manner but "not independently" (*46*). However, with hexokinase, the neutral glucose aids the binding of ATP (*48*).

In the case of the complex of hPGK with the non-natural L-ADP, there is only a small effect of PG on the k_{off} of L-ADP. We explain this by the β-phosphate of this substrate being in a different orientation to that of D-ADP, in particular, that it is further away from the 1-C of PG. It is possible that this orientation affects the relative importance of the different intermediates on the PGK reaction pathway. Any difference between the hPGK reaction pathways with D-ADP and L-ADP as the acceptor substrates could be of interest in the context of the use of L-nucleosides as prodrugs.

The different orientations of L- versus D-nucleotides when bound at the active site of other enzymes could be a general phenomenon, as it appears to be due to the inherent mirror image stereochemical characteristic of L- versus D-compounds. For example, deoxycytidine kinase is able to phosphorylate both D- and L-nucleosides because the pseudosymetry of the enantiomers, and their conformational flexibility allows a proper positioning of the 5′-hydroxyl group and the stabilization of the base in a hydrophobic pocket of the enzyme (*11, 49*). Alexandre et al. (*5*) proposed that the D/L polyvalency of UMP/CMP and dTMP kinases arises from the positional freedom of the sugar moiety that allows to keep the base and the phosphate of the two enantiomers in similar positions.

ACKNOWLEDGMENT

We are grateful to Dr. Dominique Deville-Bonne (FRE 2852, Université Paris VI) for her generous gift of the *E. coli* cells transformed with the pgk-pET28a plasmid, help in the production in purification of hPGK, and stimulating discussions. We thank Dr. Lionel Verdoucq (UMR5004, INRA Montpellier) for the use of the cell disruptor and technical advice.

REFERENCES

1. De Clercq, E. (2005) Emerging anti-HIV drugs. *Expert Opin. Emerg. Drugs 10*, 241–273.
2. De Clercq, E. (2005) Recent highlights in the development of new antiviral drugs. *Curr. Opin. Microbiol. 8*, 552–560.
3. De Clercq, E. (2005) Antiviral drug discovery and development: where chemistry meets with biomedicine. *Antiviral Res. 67*, 56–75.
4. Schlichting, I., and Reinstein, J. (1997) Structures of active conformations of UMP kinase from *Dictyostelium discoideum* suggest phosphoryl transfer is associative. *Biochemistry 36*, 9290–9296.
5. Alexandre, J. A., Roy, B., Topalis, D., Pochet, S., Périgaud, C., and Deville-Bonne, D. (2007) Enantioselectivity of human AMP, dTMP and UMP-CMP kinases. *Nucleic Acids Res. 35*, 4895–4904.
6. Scopes, R. K. (1973) 3-Phosphoglycerate kinase. *Enzymes (3rd ed.) 8*, 335–351.
7. João, H. C., and Williams, R. J. (1993) The anatomy of a kinase and the control of phosphate transfer. *Eur. J. Biochem. 216*, 1–18.
8. Mathé, C., and Gosselin, G. (2006) L-nucleoside enantiomers as antivirals drugs: a mini-review. *Antiviral Res. 71*, 276–281.
9. Coates, J. A., Cammack, N., Jenkinson, H. J., Mutton, I. M., Pearson, B. A., Storer, R., Cameron, J. M., and Penn, C. R. (1992) The separated enantiomers of 2′-deoxy-3′-thiacytidine (BCH 189) both inhibit human immunodeficiency virus replication in vitro. *Antimicrob. Agents Chemother. 36*, 202–205.
10. Schinazi, R. F., Chu, C. K., Peck, A., McMillan, A., Mathis, R., Cannon, D., Jeong, L. S., Beach, J. W., Choi, W. B., Yeola, S., and Liotta, D. C. (1992) Activities of the four optical isomers of 2′,3′-dideoxy-3′-thiacytidine (BCH-189) against human immunodeficiency virus type 1 in human lymphocytes. *Antimicrob. Agents Chemother. 36*, 672–676.
11. Sabini, E., Hazra, S., Konrad, M., Burley, S. K., and Lavie, A. (2007) Structural basis for activation of the therapeutic L-nucleoside analogs 3TC and troxacitabine by human deoxycytidine kinase. *Nucleic Acids Res. 35*, 186–192.
12. Verri, A., Montecucco, A., Gosselin, G., Boudou, V., Imbach, J. L., Spadari, S., and Focher, F. (1999) L-ATP is recognized by some cellular and viral enzymes: does chance drive enzymic enantioselectivity? *Biochem. J. 337*, 585–590.
13. Blake, C. C., and Evans, P. R. (1974) Structure of horse muscle phosphoglycerate kinase. Some results on the chain conformation, substrate binding and evolution of the molecule from a 3 angstrom Fourier map. *J. Mol. Biol. 84*, 585–601.
14. Banks, R. D., Blake, C. C. F., Evans, P. R., Haser, R., Rice, D. W., Hardy, G. W., Merrett, M., and Phillips, A. W. (1979) Sequence, structure and activity of phosphoglycerate kinase: a possible hinge-bending enzyme. *Nature 279*, 773–777.
15. Harlos, K., Vas, M., and Blake, C. C. F. (1992) Crystal structure of the binary complex of pig muscle phosphoglycerate kinase and its substrate 3-phospho-D-glycerate. *Proteins 12*, 133–144.
16. Flachner, B., Kovári, Z., Varga, A., Gugolya, Z., Vonderviszt, F., Náray-Szabó, G., and Vas, M. (2004) Role of phosphate chain mobility of MgATP in completing the 3-phosphoglycerate kinase catalytic site: Binding, kinetic, and crystallographic studies with ATP and MgATP. *Biochemistry 43*, 3436–3449.
17. May, A., Vas, M., Harlos, K., and Blake, C. (1996) 2.0 Å resolution structure of a ternary complex of pig muscle phosphoglycerate kinase containing 3-phospho-D-glycerate and the nucleotide Mn adenylylimidodiphosphate. *Proteins 24*, 292–303.
18. Szilágyi, A. N., Ghosh, M., Garman, E., and Vas, M. (2001) A 1.8 Å resolution structure of pig muscle 3-phosphoglycerate kinase with bound MgADP and 3-phosphoglycerate in open conformation: new insight into the role of the nucleotide in domain closure. *J. Mol. Biol. 306*, 499–511.
19. Kovári, Z., Flachner, B., Naray-Szabó, G., and Vas, M. (2002) Crystallographic and thiol-reactivity studies on the complex of pig muscle phosphoglycerate kinase with ATP analogues: correlation between nucleotide binding mode and helix flexibility. *Biochemistry 41*, 8796–8806.
20. Kovári, Z., and Vas, M. (2004) Protein conformer selection by sequence-dependent packing contacts in crystals of 3-phosphoglycerate kinase. *Proteins 55*, 198–209.
21. Bernstein, B. E., Michels, P. A. M., and Hol, W. G. J. (1997) Synergistic effects of substrate-induced conformational changes in phosphoglycerate kinase activation. *Nature 385*, 275–278.
22. Auerbach, G., Huber, R., Grattinger, M., Zaiss, K., Schurig, H., Jaenicke, R., and Jacob, U. (1997) Closed structure of phosphoglycerate kinase from *Thermotoga maritima* reveals the catalytic mechanism and determinants of thermal stability. *Structure 5*, 1475–1483.
23. Gallois-Montbrun, S., Faraj, A., Seclaman, E., Sommadossi, J. P., Deville-Bonne, D., and Véron, M. (2004) Broad specificity of human phosphoglycerate kinase for antiviral nucleoside analogs. *Biochem. Pharmacol. 68*, 1749–1756.
24. Krishnan, P., Gullen, E. A., Lam, W., Dutschman, G. E., Grill, S. P., and Cheng, Y. C. (2003) Novel role of 3-phosphoglycerate kinase, a glycolytic enzyme, in the activation of L-nucleoside analogs, a new class of anticancer and antiviral agents. *J. Biol. Chem. 278*, 36726–36732.
25. Varga, A., Szabó, J., Flachner, B., Roy, B., Konarev, P., Svergun, D., Závodszky, P., Périgaud, C., Barman, T., Lionne, C., and Vas, M. (2008) Interaction of human 3-phosphoglycerate kinase with L-ADP, the mirror image of D-ADP. *Biochem. Biophys. Res. Commun. 366*, 994–1000.
26. Vas, M., Merli, A., and Rossi, G. L. (1994) Antagonistic binding of substrates to 3-phosphoglycerate kinase monitored by the fluorescent analogue 2′(3′)-O-(2,4,6 trinitrophenyl)adenosine 5′-triphosphate. *Biochem. J. 301*, 885–891.
27. Merli, A., Szilágyi, A. N., Flachner, B., Rossi, G. L., and Vas, M. (2002) Nucleotide binding to pig muscle 3-phosphoglycerate kinase in the crystal and in solution: Relationship between substrate antagonism and interdomain communication. *Biochemistry 41*, 111–119.
28. Varga, A., Flachner, B., Gráczer, E., Osváth, S., Szilágyi, A. N., and Vas, M. (2005) Correlation between conformational stability of the ternary enzyme-substrate complex and domain closure of 3-phosphoglycerate kinase. *FEBS J. 272*, 1867–1885.
29. Varga, A., Flachner, B., Konarev, P., Gráczer, É., Szabó, J., Svergun, D., Závodszky, P., and Vas, M. (2006) Substrate-induced double sided H-bond network as a means of domain closure in 3-phosphoglycerate kinase. *FEBS Lett. 580*, 2698–2706.
30. Geerlof, A., Schmidt, P. P., Travers, F., and Barman, T. (1997) Cryoenzymic studies on yeast 3-phosphoglycerate kinase. Attempt to obtain the kinetics of the hinge-bending motion. *Biochemistry 36*, 5538–5545.
31. Geerlof, A., Travers, F., Barman, T., and Lionne, C. (2005) Perturbation of yeast 3-phosphoglycerate kinase reaction mixtures with ADP: transient kinetics of formation of ATP from bound 1,3-bisphosphoglycerate. *Biochemistry 44*, 14948–14955.
32. He, J., Roy, B., Périgaud, C., Kashlan, O. B., and Cooperman, B. S. (2005) The enantioselectivities of the active and allosteric sites of mammalian ribonucleotide reductase. *FEBS J. 272*, 1236–1242.
33. Schmidt, P. P., Travers, F., and Barman, T. (1995) Transient and equilibrium kinetic studies on yeast 3-phosphoglycerate kinase. Evidence that an intermediate containing 1,3-bisphosphoglycerate accumulates in the steady state. *Biochemistry 34*, 824–832.
34. Sali, A., and Blundell, T. L. (1993) Comparative protein modelling by satisfaction of spatial restraints. *J. Mol. Biol. 234*, 779–815.
35. Humphrey, W., Dalke, A., and Schulten, K. (1996) VMD: visual molecular dynamics. *J. Mol. Graph. 14*, 33–38.
36. Davies, G. J., Gamblin, S. J., Littlechild, J. A., Dauter, Z., Wilson, K. S., and Watson, H. C. (1994) Structure of the ADP complex of the 3-phosphoglycerate kinase from *Bacillus stearothermophilus* at 1.65 Å. *Acta Crystallogr. D50*, 202–209.
37. Brooks, B., Bruccoleri, R., Olafson, B., States, D. S. S., and Karplus, M. (1983) CHARMM: a program for macromolecular energy, minimization and molecular dynamics calculations. *J. Comput. Chem. 4*, 187–217.

38. Scopes, R. K. (1978) Binding of substrates and other anions to yeast phosphoglycerate kinase. *Eur. J. Biochem. 91*, 119–129.
39. Johnson, P. E., Abbott, S. J., Orr, G. A., Sémériva, M., and Knowles, J. R. (1976) The "phosphoryl-enzyme" from phosphoglycerate kinase. *Biochemistry 15*, 2893–2901.
40. Douzou, P. (1977) Enzymology at subzero temperatures. *Adv. Enzymol. Relat. Areas Mol. Biol. 45*, 157–272.
41. Gutfreund, H. (1995) *Kinetics for the Life Sciences*, Cambridge University Press, Cambridge.
42. Koshland, D. E., Jr (1956) Molecular geometry in enzyme action. *J. Cell. Physiol. Suppl. 47*, 217–234.
43. Gutfreund, H. (1987) Reflections on the kinetics of substrate binding. *Biophys. Chem. 26*, 117–121.
44. Cserpán, I., and Vas, M. (1983) Effects of substrates on the heat stability and on the reactivities of thiol groups of 3-phosphoglycerate kinase. *Eur. J. Biochem. 131*, 157–162.
45. Vas, M., and Batke, J. (1984) Adenine nucleotides affect the binding of 3-phosphoglycerate to pig muscle 3-phosphoglycerate kinase. *Eur. J. Biochem. 139*, 115–123.
46. Deville-Bonne, D., Laine, R., and Garel, J. R. (1991) Substrate antagonism in the kinetic mechanism of *E. coli* phosphofructokinase-1. *FEBS Lett. 290*, 173–176.
47. Zheng, R. L., and Kemp, R. G. (1992) The mechanism of ATP inhibition of wild type and mutant phosphofructo-1-kinase from *Escherichia coli*. *J. Biol. Chem. 267*, 23640–23645.
48. Viola, R. E., Raushel, F. M., Rendina, A. R., and Cleland, W. W. (1982) Substrate synergism and the kinetic mechanism of yeast hexokinase. *Biochemistry 21*, 1295–1302.
49. Sabini, E., Hazra, S., Konrad, M., and Lavie, A. (2007) Nonenantioselectivity property of human deoxycytidine kinase explained by structures of the enzyme in complex with L- and D-nucleosides. *J. Med. Chem. 50*, 3004–3014.

BI7023145